Structural Changes as a Result of Processing in Thermoplastic Bloodmeal

Casparus J. R. Verbeek,[1] Lisa E. van den Berg[2]

[1]*University of Waikato, School of Engineering, Hamilton, New Zealand*
[2]*WaikatoLink, Hamilton, New Zealand*

Received 19 October 2010; accepted 8 February 2012
DOI 10.1002/app.36964
Published online in Wiley Online Library (wileyonlinelibrary.com).

ABSTRACT: Bloodmeal (BM) can be thermoplastically processed resulting in a material with good mechanical properties by using a correct combination of additives. In this article, combinations of water, sodium sulfite (SS), sodium dodecyl sulfate (SDS), and urea were compounded with BM, and water absorption, solubility, thermal stability, and protein secondary structure were assessed. Thermal stability of processed plastics was reduced when using 2 or 3 pph_{bm} (parts per hundred parts BM) SS and 20 pph_{bm} urea, mostly indicative of a reduction in covalent crosslinking. SS was required for chain mobility during processing, however, without sufficient plasticization degradation will occur instead of melt formation. SDS further improved processability and consolidation leading to increased water absorption and solubility, indicative of a reduction in chain interactions. It was found that BM proteins are highly denatured and thermoplastic processing reduced ordered structures further. Additional minor structural changes occurred as a result of reduced covalent and noncovalent interactions after processing. It was concluded that the increase in water absorption and solubility was due to changes in intermolecular and intramolecular interactions, rather than substantial structural changes. © 2012 Wiley Periodicals, Inc. J Appl Polym Sci 000: 000–000, 2012

Key words: extrusion; biopolymers; crosslinking

INTRODUCTION

In contrast to the number of studies on the production of bioplastics from soy and wheat proteins, little has been studied regarding animal proteins like bloodmeal (BM). In a previous study, it has been shown that BM can be extruded and injection molded using chemical additives. These were required to break covalent crosslinks, intermolecular, and intramolecular forces, such as hydrophobic and hydrogen bonding as well as to plasticizing the protein chains.[1]

It is understood that molecular organization and structural characteristics of polymers influence the material's final properties.[2] The combination of heat, pressure, shear, and chemical additives will affect chain alignment as well as intermolecular and intramolecular interactions. Secondary structural patterns of proteins are characterized by periodic structures such as, helices, sheets, and extended portions, as well as a variety of turns, loops, and disordered coils[3] and can be determined using Fourier transform infrared spectroscopy (FTIR) spectroscopy. Secondary structure are often assessed based on a protein's absorption in the amide I region (1600–1700 cm^{-1}).[3–8]

The amide I absorption contains contributions from the C=O stretching vibration of the amide group (~ 80%) with a minor contribution from the C—N stretching vibration.[8] Each secondary structure, helix, β-sheet, β-turn, and unordered give rise to somewhat different C=O stretching frequencies due to their unique molecular geometry and hydrogen bonding pattern.[7,8] Stronger hydrogen bonding involving the amide C=O, results in a lower electron density in the C=O group causing amide I absorption at lower frequencies.[8] Structures involving extended sheets have shorter and stronger hydrogen bonds compared to helices and will therefore have a lower amide I absorption frequency.[8]

Absorption peaks of various secondary structures overlap within the amide I region and often result in a featureless absorption spectra.[8] To overcome this, overlapping peaks of the spectra need to be revealed by techniques such as Fourier self deconvolution (FSD) and second derivatives. To avoid artifacts due to data processing, only features present in both derivative and deconvolved spectra should be used for quantitative analysis.[8]

Although the native secondary structure is denatured during thermoplastic processing, secondary structure elements may contribute to physical fixation as the processed material cools.[9] Changes to secondary structure induced by thermoplastic processing

Correspondence to: C. J. R. Verbeek (jverbeek@waikato.ac.nz).

Contract grant sponsors: WaikatoLink Ltd.

depend on the protein's primary structure, processing conditions and additives such as plasticizers or denaturing agents. In general, extrusion appears to favor an increase in ordered β-sheet regions at the expense of α-helices, but this is not always the case.[10] Time-resolved FTIR of soybean protein films held at 100°C showed changes in the amide I region over time that may be attributed to an increase in β-turn or weak β-sheet structures.[11]

Amide I analysis of hot pressed films of egg albumin, lactalbumin, feather keratin, and wheat gluten suggested increased order in the form of β-sheets as glycerol content increased up to a critical value for each protein. Beyond this, critical value order decreased.[12] FTIR analysis of film blown thermoplastic zein plasticized with polyethylene glycol highlighted the interdependence of structure and processing. Different batches of zein powder contained different ratios of β-sheets to α-helices, and the best blown films were prepared from those with largest relative α-helical content. In turn, the processing increased the α-helical content and decreased the presence of ordered β-sheet regions.[13] Crosslinks induced by γ-radiation in whey, casein, and soya films appeared to have reduced β-sheet regions.[13]

Other analysis techniques could also be useful to assist in interpreting structural changes during processing. Solubility of protein bioplastics before and after processing is often regarded as a good indicator of crosslink formation during processing.[14,15]

Water absorption is a qualitative test for analyzing the crosslink density of protein bioplastics, which can be related to mechanical properties.[16,17] A decrease in water absorption can often be attributed to increased protein interactions after denaturing, but high temperatures may also lead to degradation which could result in a increase in water absorption.[16]

Water absorption is not only influenced by covalent crosslinking but also by the proteins ability to interact with water. Exposing hydrophobic groups, either by chain rearrangement or by chemical additives may also influence water absorption. However, in the absence of these additives, water absorption could be considered proportional to crosslink density, for most protein plastics.

The objective of this study was to assess changes in BM's secondary structure as a result of thermoplastic processing using different combinations of sodium sulfite (SS), urea, sodium dodecyl sulfate (SDS), and water.

MATERIALS AND METHODS

Materials

BM was obtained in powder form from Taranaki By-Products, New Zealand, and sieved to an average particle size of 700 μm. Technical grade SDS was obtained from Biolab (NZ), analytical grade SS from BDH Lab Supplies, and agricultural grade urea from Balance Agri-Nutrients (NZ).

TABLE I
Taguchi L8 Fractional Factorial Design

Exp	Urea (pph_{bm})	SDS (pph_{bm})	SS (pph_{bm})	Water (pph_{bm})
1	10	0	1	45
2	20	3	1	45
3	20	0	1	60
4	10	3	1	60
5	20	0	3	45
6	10	3	3	45
7	10	0	3	60
8	20	3	3	60

pph_{bm}, parts per hundred bloodmeal.

Method

The Taguchi method uses orthogonal arrays in its experimental design.[18] Following from scoping trials, it was possible to construct an L8 fractional factorial experimental design to assess the relative effect of each additive on water absorption solubility and changes in secondary structure, as outlined in Table I. The analysis was performed in triplicate for each specimen produced.

The results of the Taguchi experiment are analyzed in two steps: first, the influence and main effects of each factor are qualitatively assessed. Second, analysis of variance (ANOVA) is used to quantify the relative influence of each factor. A 95% confidence interval was used in all analyses.

Samples were prepared by dissolving all additives in the appropriate amount of water followed by blending with BM powder in a high-speed mixer. The mixtures were stored for at least 1 h before extrusion.

Extrusion trials were performed using a ThermoPrism TSE-16-TC twin-screw extruder at a screw speed of 150 rpm, and a temperature profile and screw configuration shown in Figure 1. Actual melt temperatures were within 2–5°C of the set temperatures. The extruder had a screw diameter of 16 mm, an L/D ratio of 25, and was fitted with a single 10-mm circular die. A relative torque of 50–60% of the maximum allowed in the extruder was maintained (12 Nm per screw maximum), by adjusting the mass flow rate of the feed. The extruder was fed by an oscillating trough and the extruded material was granulated using a tri-blade granulator from Castin Machinery Manufacturer, New Zealand, over a 4-mm mesh. Samples were injection molded directly after extrusion and granulation, without further conditioning.

Injection-molded specimens were produced using a 22-mm screw diameter BOY 15 S injection molding

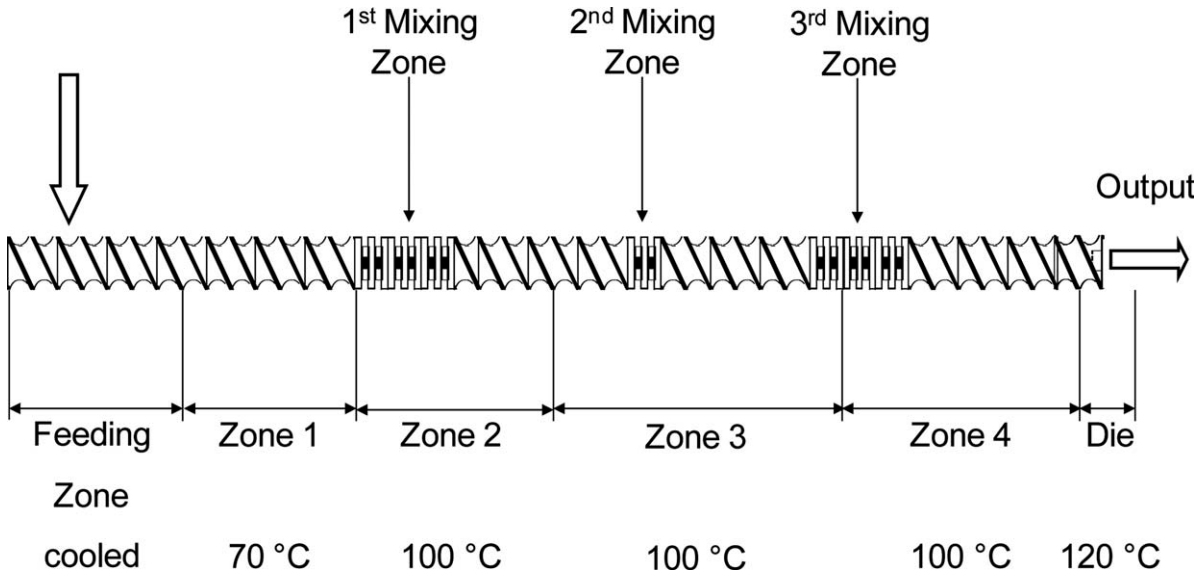

Figure 1 Extruder screw configuration and corresponding temperature profile.

machine. Specimens were injected through a cold runner into a water-heated mold. The shape of the tensile test specimens was in accordance with ASTM D638. A temperature profile of 70 (feed zone), 115, and 120°C (die zone) was used using 1200 bar injection pressure and 400 bar back pressure at screw speed of 150 min^{-1}. A 20-s cooling time was allowed in a mold locked with 30-kN locking force.

Analysis

Moisture content

Moisture content was determined gravimetrically by weighing ~ 1.5-g granulated material ($M_{initial}$) into aluminum dishes, followed by drying (M_{dry}) in an air-circulating oven at 100°C for 12+ h. Percentage moisture content $\left(M_c = \frac{M_{dry} - M_{initial}}{M_{dry}}\right) \times 100$ was done in triplicate for each experiment.

Water absorption and solubility

Extruded samples were granulated, weighed, and immersed in distilled water for 24 h at 20°C. Surface water was removed using a paper towel before weighing. The samples were then dried at 100°C for 12+ h and reweighed. The difference between the initial mass ($M_{initial}$) and mass after immersion (M_{wet}) was used to calculate percentage water absorption $\left(\% \text{ water absorbtion} = \frac{M_{wet} - M_{initial}}{M_{initial}}\right) \times 100$. The difference between the dry mass (M_{dry}) and the dry mass after water immersion (M_{after}) was used to calculate the percentage solubility of $\left(\% \text{ solubility} = \frac{M_{dty} - M_{after}}{M_{dry}}\right) \times 100$. Materials were tested after extrusion as well as after injection molding, and an average of three specimens is presented.

Thermogravimetric analysis. Approximately 10 mg of dried and ground sample was scanned using simultaneous differntial scanning calorimetery/thermogravimetric analysis (SDT 2960, TA Instruments, New Castle, DE) from room temperature to 500°C at a rate of 10°C min^{-1}.

Fourier transform infrared spectroscopy. Freeze-dried and powderized samples were prepared as KBr pellets (1 mg sample and 100 mg salt). The FTIR spectra were recorded using a Perkin-Elmer spectrophotometer with 16 scans at 4 cm^{-1} resolution, from 4000 to 400 cm^{-1}. Three specimens were prepared for each sample, and the FTIR scan was repeated three times. A background scan was performed before each sample scan and subtracted from each sample spectra automatically by the FTIR software.

In this study, the corresponding peaks of the FSD curve (half width = 13 cm^{-1}) and the second derivative (1.2% smoothing) were used to quantify the structural parameters, using Peak Fit v4.12 with 65% filtering between 900 and 2100 cm^{-1}.[19]

Using the AutoFit II second derivative function (Gaussian area), corresponding component peaks between the second derivative and the FSD curve were selected. Using PeakFit v4.12, a least squares curve fitting function was used to reproduce the experimentally obtained amide I composite peak by adjusting individual component peak areas until the total is approximately the experimental area under the amide I composite profile.[19] Individual area estimates were used to manually calculate the relative amounts of helices (α-helix and 3_{10}-helix), β-sheets, β-turns, and unordered structures, each corresponding to a specific wavelength (Table II).

TABLE II
Correlations between Common Protein Structures and Amide I Frequency[8]

Structure	Amide I frequency (cm^{-1})
Intermolecular β-sheet	1610–1628
Intramolecular β-sheet	1625–1640
Unordered	1640–1648
α-helix	1648–1658
α_{10}-helix	1660–1670
β-turns	1675–1695

X-Ray diffraction. Changes in morphology were measured using wide angle powder X-ray diffraction (XRD), using a Phillips X'Pert machine using CuKα radiation at 40 kV and 40 mA. Diffraction patterns were collected using a counting time of 4 s $step^{-1}$ and a step size of 0.02° with a receiving slit height of 0.5 mm, and the data was collected between 1 and 70° 2θ.

RESULTS AND DISCUSSION

Water absorption and solubility

Water absorption and solubility results are presented in Table III. ANOVA was used to analyze the results after extrusion, injection molding as well as the relative change between them. Also shown in Table III, are the material's moisture content of the original formulation, after extrusion and after injection molding. The results indicate that some moisture has been lost as a result of processing which may affect rheological properties as well as material properties such as strength, Young's modulus and the glass transition temperature. However, when those are measured, materials are typically conditioned under a standard atmosphere to account for moisture loss during processing. For the properties measured in this study, small changes in moisture during processing was not important. Other additives are not expected to change as these are nonvolatile.

From Figure 2, it can be seen that SDS and SS had the largest effect on water absorption when tested after extrusion. Increasing SS or SDS from Level 1 to Level 2 increased water absorption. It was concluded that the disulfide cleavage action of SS and hydrophobic bonding restriction of SDS led to chain rearrangement thereby exposing hydrophilic groups which increased water absorption.

Water absorption after injection molding was clearly higher than after extrusion. From Figure 2, it can be seen that SS was the only statistically significant factor at 67%. To further investigate the effect of injection molding, the difference between extrusion and injection molding was analyzed in a similar fashion and is presented in Figure 2. Urea and the interaction between SS and water were the only significant factors. Materials containing 20 pph_{bm} urea (Level 2) had higher water absorption due to the increased prevention of secondary interactions between chains and also because urea is hydrophilic.

The significance of the interaction between SS and water suggests that a reducing agent is required in conjunction with water to enable chain mobilization. Samples containing 3 pph_{bm} SS (Level 2) and 45 pph_{bm} water (Level 1) had a greater increase in water absorption after injection molding. This was attributed to mechanical degradation of the polymer at low water levels (high viscosity). About 3 pph_{bm} SS (Level 2) and 60 pph_{bm} water (Level 2) resulted in the smallest increase in water absorption after injection molding, attributed to high unfolding and alignment of chains. SS at 1 pph_{bm} was insufficient to break all covalent crosslinks, resulting in reduced chain mobility.

Solubility

Because urea is water soluble, the measured solubility was corrected by subtracting the amount of urea from the solubility of extruded and injection-molded samples. The difference between the solubility of extruded and injection-molded samples was calculated using the corrected data, assuming that all the urea present was solubilized. SS and SDS were the most significant factors affecting solubility after extrusion and injection molding (Fig. 2). The addition of SDS

TABLE III
Moisture Content, Water Absorption, and Solubility before and after Extrusion and Injection Moulding

	Moisture content			Water absorption		Solubility	
Exp #	Original (wt %)	Extrusion (wt %)	Injection (wt %)	Extrusion (wt %)	Injection (wt %)	Extrusion (wt %)	Injection (wt %)
1	28.6	25.8	23.6	30.6	135.6	7.7	8.7
2	26.6	24.8	23.5	57.8	323.7	13.6	18.7
3	33.2	29.8	27.6	20.8	197.4	12.1	13.9
4	34.3	31.3	31.3	47.2	214.0	7.8	10.2
5	27.0	24.8	17.8	69.7	692.3	14.5	27.1
6	27.7	25.5	21.2	102.1	717.4	10.8	25.3
7	34.1	29.6	26.7	71.0	335.0	9.0	13.3
8	32.0	28.9	26.3	123.4	737.5	14.9	26.0

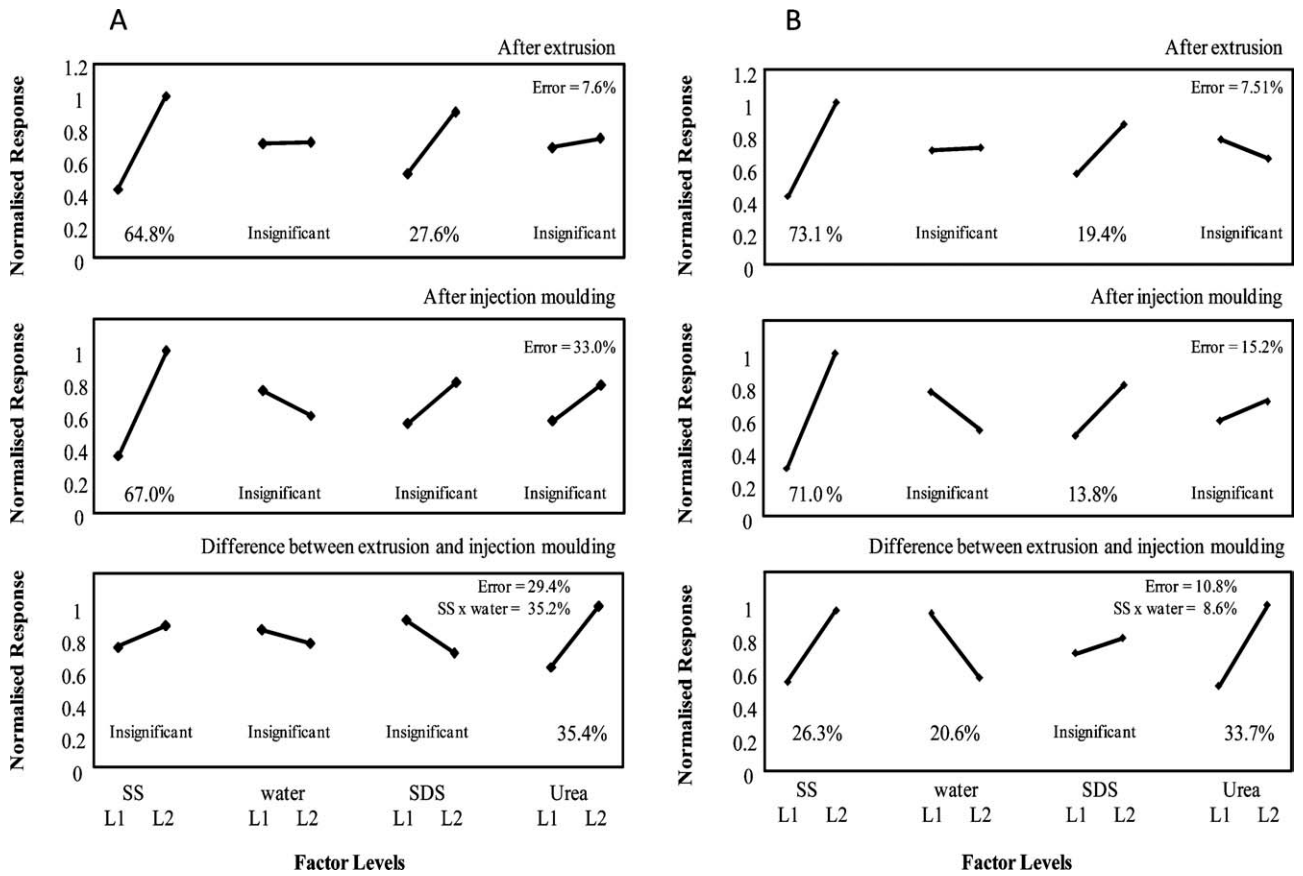

Figure 2 Main effects (normalized response) and ANOVA results for (A) water absorption and (B) solubility tests.

reduces hydrophobic interactions resulting in a more soluble material through unfolding of protein chains. SS at 3 pph_{bm} (Level 2) resulted in higher solubility, provided sufficient plasticizer was also used.

Generally, solubility after extrusion was less than after injection molding. Furthermore, the water color of injection-molded samples were significantly more red compared to extruded samples, suggesting the hemoglobin or fractions thereof became more soluble. This was further investigated to determine whether the added pressure during injection molding, or a combination of added pressure and the chemical additives was the main cause for this observation. To do this, the percent change between the solubility of extruded and injection-molded samples was calculated and analyzed using ANOVA (Fig. 2).

SS, water, and urea were the most significant factors on the change in solubility after injection molding. Increasing the concentration of SS and urea increased the change in solubility after injection molding. This was expected as the added pressure during injection molding will enhance the denaturing ability of these chemicals.

Water content was found to be an important factor influencing the solubility difference between extruded and injection-molded samples. From Figure 2, it can be seen that increasing water content resulted in a smaller increase in solubility after injection molding. Using water at Level 1 required greater injection pressure resulting in protein degradation. The interaction between SS and water further supports this finding. Increased degradation (increased redness of solvent) was observed for samples with Level 1 water (Experiments 1, 2, 5, and 6).

Water absorption and solubility results were closely related; 3 pph_{bm} SS and 3 pph_{bm} SDS were required for effective chain mobility during processing, by reducing secondary interactions. To avoid protein degradation during injection molding, sufficient water should be used to allow plasticization. The addition of 20 pph_{bm} urea also increased chain mobility and prevented secondary interactions, resulting in higher water absorption and solubility. Unexpectedly, the combination of 3 pph_{bm} SS and 60 pph_{bm} water resulted in smaller increase of water absorption and solubility after injection molding when compared with 45 pph_{bm} water at the same SS content. This was attributed to high chain mobilization, which allowed increased secondary interactions.

Secondary structure

Bovine blood consists mainly of hemoglobin, serum albumin, globulins, and fibrinogen, with an overall

TABLE IV
Quantitative Analysis of Secondary Structures in Unprocessed Blends of Urea and BM

		Secondary structure feature (mol %)			
BM (wt %)	Urea (wt %)	Helix	Beta sheet	Beta turns	Unordered
100%	***0%***	***29.0%***	***27.5%***	***27.7%***	***15.8%***
95%	5%	27.9%	28.5%	28.3%	15.3%
90%	10%	27.3%	30.2%	27.4%	15.1%

α-helix content of about 62%.[20] When BM is produced, heating results in protein denaturation and water is evaporated leaving dehydrated polymer chains. Secondary structures that have been assigned to specific absorption frequencies within the amide I region are shown in Table II.[4,8,21,22] It was found that BM contained only 29% α-helices, indicative of a highly denatured structure. The removal of protein–water interactions increased protein–protein interactions, allowing close packing of protein chains in the β-sheet conformation, which is consistent with other studies.[23–25]

FTIR spectra of proteins can be affected by substances such as water and urea which absorbs strongly in the amide I region.[7,26] In this study, the effect of water was minimized by freeze-drying samples before testing and by water-vapor background subtraction. To account for urea, nonmelt processed mixtures of 5 and 10% freeze-dried urea in freeze-dried BM as well as pure freeze dried urea were prepared and analyzed according to the same methods used for the plasticized samples. Urea in KBr absorbs at $\sim$ 1605, 1632, and 1685 cm^{-1}. In theory, these absorbencies would show up as an increase in β-sheet (1626–1640 cm^{-1}) and β-turns (1675–1695 cm^{-1}). From Table IV, it can be seen that increasing urea content resulted in an apparent increase in β-structure content. The change in structural features was taken into account by subtracting the contribution of urea (Table IV) for each structural feature for nonmelt processed blends from that of extruded samples.

Effect of processing on secondary structure

It was found that compared to neat BM, there was generally a decrease in helix and β-sheet accompanied by an increase in β-turns and unordered structures when using the additives, as outlined in Table V. Because of small changes and uncertainty of structural assignments above 1660 cm^{-1}, ordered structures were considered together, as helices, β-sheets and β-turns in subsequent statistical analysis.

It was observed that the most significant structural changes occurred after injection molding and subsequent statistical analysis were based in the relative change in secondary structure between extrusion and injection molding. It can be seen from Table V that generally, there was an increase in ordered structures after injection molding. The only exception to this observation was Experiments 7 and 8 where SS and water were used at Level 2. The main effects and ANOVA results are presented in Figure 3.

From Figure 3, it can be seen that SS has the largest percentage contribution to the main effect. Ordered structures were reduced by the combined action of SS at Level 2 and the more aggressive conditions of injection molding. When excessive covalent disulfide bonds are present with SS at Level 1, chain mobilization is restricted, forcing chains to form more thermally stable localized interactions leading to a more ordered structure.

It can be observed that by increasing urea concentrations the amount of ordered structure was also reduced. This can be explained by the fact that helix and β-sheet structures rely on hydrogen bonding,

TABLE V
Structural Changes after Extrusion and Injection Moulding

	Extruded				Injection molded				
Exp #	Helix (%)	β-sheet (%)	β-Turns (%)	Unordered (%)	Helix (%)	β-sheet (%)	β-Turns (%)	Unordered (%)	Δ (%)[a]
1	23.1	25.1	31.6	20.2	25.3	27.4	30.4	16.9	4.1
2	24.9	24.5	32.3	18.3	26.8	26.7	30.4	16.2	2.6
3	24.2	26.5	32.5	16.9	29.5	26.1	28.9	15.5	1.6
4	24.6	23.7	31.7	20.0	26.5	25.8	30.9	16.7	4.1
5	26.6	27.5	30.5	15.4	29.0	26.5	29.1	15.4	0.1
6	21.2	27.6	33.7	17.5	28.4	26.9	28.7	16.0	1.8
7	25.5	24.7	31.3	18.4	25.8	23.7	30.3	20.7	−2.8
8	29.8	27.1	27.9	15.1	18.8	29.6	33.8	17.7	−3.0

[a] Δ(%) = (ordered structure after extrusion − ordered structure after injection moulding/ordered structure after extrusion).

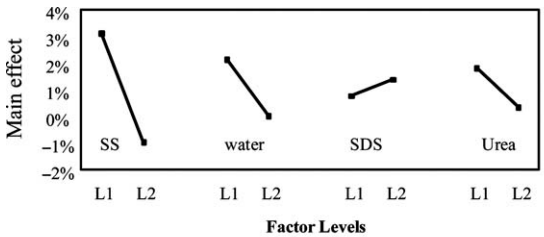

ANOVA Analysis

	DOF	*F*	*Percentage Contribution*
SS	1	78.8	62.0%
Water	1	21.5	17.0%
SDS	Factor Pooled		
Urea	1	10.5	8.2%
SS x Water	1	13.2	10.4%
SS x SDS	Factor Pooled		
SS x Urea	Factor Pooled		
Error	3		2.4%
$F_{1,3} = 5.5383$			
Total	7		100%

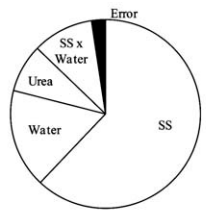

Figure 3 Percentage change in ordered structures; main effects and ANOVA.

which is disrupted by urea, resulting in more unordered structures.

When seen in light of results concerning water absorption and solubility, the importance of the combination of SS and water is highlighted. SS at Level 2 and water at Level 1 led to degradation as opposed to chain mobilization. The interaction between SS and water further supported this; using SS at Level 2 and water at Level 1, materials had a highly ordered structure compared to using SS and water both at Level 2. Furthermore, at higher water content, the plasticization effect of water will increase free volume and chain mobility leading to a more unordered structure after injection molding. However, short peptides, as a result of degradation, can also form local hydrogen bonds, resulting in the thermodynamically stable helix structure. The overall result was an observed increase in ordered structure at Level 1 water.

The formation of ordered structures requires stabilization by secondary interactions, like hydrogen bonding. Increased chain mobility and decreased secondary interactions will therefore favor unordered structures. The increase in unordered structure, when using SS and water at Level 2, may explain the increase in water absorption, because less chain entanglements and interactions can occur between chains.

Structural changes due to processing were small compared to change in secondary structure of native blood proteins upon drying. The chemical additives had an influence on reducing ordered structures by altering the intermolecular and intramolecular interactions. Injection-molded samples with SS and water at Level 2 was highly plasticized and was the only samples with decreased ordered structure after injection molding. Increased plasticization resulted in an increase in chain mobility and reduction in protein–protein interactions, therefore reducing the amount of ordered structures. These results were further supported by XRD, as shown in Figure 4.

From Figure 4, it can be seen that BM showed a strong peak at about 10 and 20° 2θ. A decrease in intensity and a broadening of the peak at 20° is often taken as an indication of a reduction in crystal size.[27] In all cases investigated here, processing

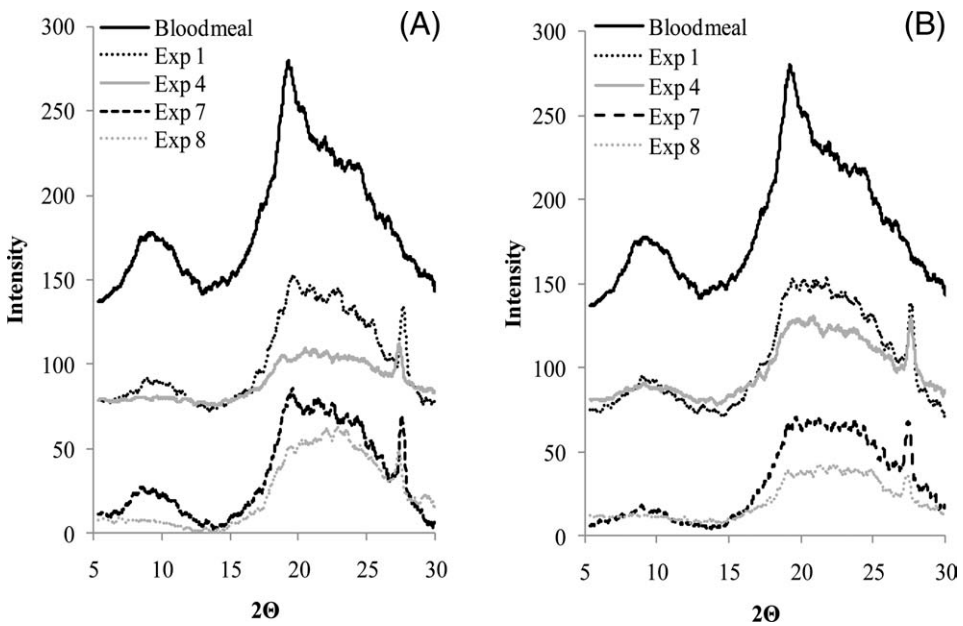

Figure 4 XRD patterns for bloodmeal as well as patterns for selected extruded (A) and injection-molded (B) samples.

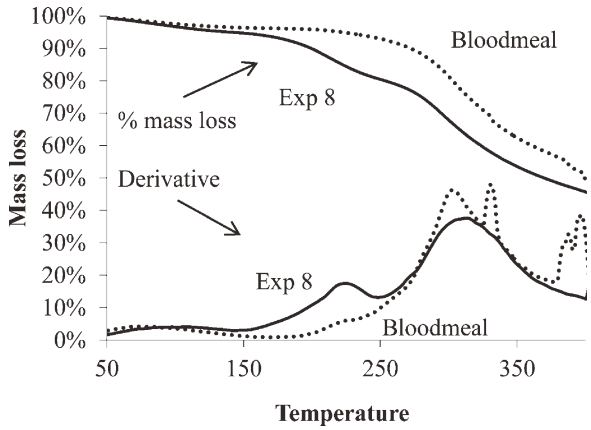

Figure 5 Thermal degradation of bloodmeal and material from Experiment 8.

resulted in a reduction in intensity and peak broadening. Results also suggest that the materials that were thought to have more unordered structures according to FTIR analysis, showed an increase in amorphous behavior, which is consistent with a diminishing peak at about 10°.[12]

Thermal degradation

Generally, the onset of thermal degradation for crosslinked polymers is at higher temperatures than noncrosslinked polymers. TGA is an effective method to analyze thermal stability, potentially providing information on secondary interactions.

Thermal degradation of BM-plastics occurred in four steps: 0–150°C, 150–230°C, 230–380°C, and above 380°C (Fig. 5). Up to 150°C, there was an average loss of 4.5 wt %, attributed to the evaporation of bound water. The second step was attributed to the degradation of urea. The region between 230 and 380°C was credited to cleavage of S—S, O—N, and O—O linkages. The final step was attributed thermal decomposition, through peptide bond reduction. Previous research on protein-based bioplastics showed similar thermal degradation behavior.[28–32]

It was found that BM was more thermally stable compared to processed BM-plastics, and therefore, it was concluded that BM had the highest degree of crosslinking. The degradation of crosslinks would occur between 230 and 380°C and the inflection point in the percent mass loss versus temperature curve was used for comparative processes.

Increasing the level of either SS or urea reduced the onset of thermal degradation, which implied a reduction in thermal stability. These results were consistent with earlier observations where it was concluded that SS and urea reduced crosslinking (either physical or chemical) by their combined effect on chain mobility, secondary interactions, and covalent bonding.

CONCLUSIONS

The aim of this study was to investigate structural changes and intermolecular/intramolecular interactions as a result of thermoplastic processing of BM. Extrusion and injection molding were used to produce biopolymers based on BM and appropriate chemical additives.

SS and SDS were the most important factors leading to increased water absorption and solubility after processing. Increased water redness was observed after injection molding which was attributed to the interaction between SS and water. Protein degradation occurred at the combination of high SS and low water levels compared to chain mobilization at higher water contents.

Plasticized polymers had a less ordered structure compared to BM. However, an increase in order was observed between injection-molded samples and extruded samples, except when SS and water were both at higher levels. SS, water, and their interaction were the most important factors affecting structural changes. In the absence of sufficient plasticizers, the addition of SS also led to degradation during processing, as opposed to melt formation. It was concluded that the increase in processability, consolidation, water absorption, and solubility was due to changes in intermolecular and intramolecular interactions, rather than substantial structural changes.

Successful processing of proteins using extrusion requires increased chain mobility. This was achieved with BM by using SS, water, SDS, and urea at Level 2. At this composition, intermolecular and intramolecular interactions were reduced shown by the increase in processability, consolidation, and water absorption. This reduction in macromolecular interactions resulted in decreasing the amount of ordered structures.

References

1. Verbeek, C.; van den Berg, L. J Polym Environ 2010, 1.
2. Cuq, B.; Gontard, N.; Guilbert, S. Cereal Chem 1998, 75, 1–9.
3. Kumosinski, T. F.; Farrell, H. M., Jr. Trends Food Sci Technol 1993, 4, 169.
4. Zhao, X.; Chen, F.; Xue, W.; Lee, L. Food Hydrocolloid 2008, 22, 568.
5. Yu, P.; McKinnon, J. J.; Christensen, C. R.; Christensen, D. A. J Agric Food Chem 2004, 52, 7353.
6. Surewicz, W. K.; Mantsch, H. H.; Chapman, D. Biochemistry 1993, 32, 391.
7. Kong, J.; Yu, S. Acta Biochim Biophys Sin 2007, 39, 549.
8. Jackson, M.; Mantsch, H. H. Crit Rev Biochem Mol Biol 1995, 30, 95.
9. De Graaf, L. A. J Biotechnol 2000, 79, 299.
10. Verbeek, C. J. R.; van den Berg, L. E. Macromol Mater Eng 2009, 295, 10.
11. Tian, K.; Porter, D.; Yao, J.; Shao, Z.; Chen, X. Polymer 2010, 51, 2410.

12. Athamneh, A. I.; Griffin, M.; Whaley, M.; Barone, J. R. Biomacromolecules 2008, 9, 3181.
13. Oliviero, M.; Maio, E. D.; Iannace, S. J Appl Polym Sci 2010, 115, 277.
14. Mohammed, Z. H.; Hill, S. E.; Mitchell, J. R. J Food Sci 2000, 65, 221.
15. Camire, M. J Am Oil Chem Soc 1991, 68, 200.
16. Huang, H. C.; Chang, T. C.; Jane, J. J Am Oil Chem Soc 1999, 76, 1101.
17. Pommet, M.; Redl, A.; Guilbert, S.; Morel, M.-H. J Cereal Sci 2005, 42, 81.
18. Roy, R. A Primer on the Taguchi Method; Society of Manufacturing Engineers: Dearborn, Michigan, 1990.
19. PeakFit v4.12; SeaSolve Software Inc.: Framingham, MA, 2003.
20. Bhattacharyya, J.; Bhattacharyya, M.; Chakraborti, A. S.; Chaudhuri, U.; Poddar, R. K. Int J Biol Macromol 1998, 23, 11.
21. Pelton, J. T.; McLean, L. R. Anal Biochem 2000, 277, 167.
22. Maury, M.; Murphy, K.; Kumar, S.; Mauerer, A.; Lee, G. Eur J Pharm Biopharm 2005, 59, 251.
23. Yuryev, V. P.; Zasypkin, D.; Tolstoguzov, V. B. Die Nahrung 1990, 34, 607.
24. Weegels, P. L.; Verhoek, J. A.; de Groot, A. M. G.; Hamer, R. J. J Cereal Sci 1994, 19, 31.
25. Subirade, M.; Kelly, I.; Guéguen, J.; Pézolet, M. Int J Biol Macromol 1998, 23, 241.
26. Iloro, I.; Goñi, F. M.; Arrondo, J. L. R. Acta Biochim Polym 2005, 52, 477.
27. Saiah, R.; Sreekumar, P. A.; Leblanc, N.; Saiter, J. M. Ind Crops Prod 2009, 29, 241.
28. Liu, D.; Zhang, L. Macromol Mater Eng 2006, 291, 820.
29. Nanda, P. K.; Rao, K. K.; Nayak, P. L. J Appl Polym Sci 2007, 103, 3134.
30. Leblanc, N.; Saiah, R.; Beucher, E.; Gattin, R.; Castandet, M.; Saiter, J.-M. Carbohydr Polym 2008, 73, 548.
31. Schmidt, V.; Giacomelli, C.; Soldi, V. Polym Degrad Stab 2005, 87, 25.
32. Jerez, A.; Partal, P.; Martínez, I.; Gallegos, C.; Guerrero, A. Rheol Acta 2007, 46, 711.